arXiv:0805.4642v3 [hep-ph] 25 Sep 2009

Macroscopic Strings and "Quirks" at Colliders

Junhai Kang,[a] Markus A. Luty,[a,b]

[a] *Physics Department, University of Maryland*
College Park, Maryland 20742

[b] *Physics Department, University of California Davis*
Davis, California 95616

Abstract

We consider extensions of the standard model containing additional heavy particles ("quirks") charged under a new unbroken non-abelian gauge group as well as the standard model. We assume that the quirk mass m is in the phenomenologically interesting range 100 GeV–TeV, and that the new gauge group gets strong at a scale $\Lambda < m$. In this case breaking of strings is exponentially suppressed, and quirk production results in strings that are long compared to Λ^{-1}. The existence of these long stable strings leads to highly exotic events at colliders. For 100 eV $\lesssim \Lambda \lesssim$ keV the strings are macroscopic, giving rise to events with two separated quirk tracks with measurable curvature toward each other due to the string interaction. For keV $\lesssim \Lambda \lesssim$ MeV the typical strings are mesoscopic: too small to resolve in the detector, but large compared to atomic scales. In this case, the bound state appears as a single particle, but its mass is the invariant mass of a quirk pair, which has an event-by-event distribution. For MeV $\lesssim \Lambda \lesssim m$, the strings are microscopic, and the quirks annihilate promptly within the detector. For colored quirks, this can lead to hadronic fireball events with $\sim 10^3$ hadrons with energy of order GeV emitted in conjunction with hard decay products from the final annihilation.

1 Introduction

The LHC has energized the particle physics community with the promise of new physics at the TeV scale. This is the scale where the origin of electroweak symmetry breaking and the solution of the hierarchy problem must lie. Most studies of physics beyond the standard model therefore involve minimal models directly motivated by these problems, most notably the MSSM. However, history teaches us that the true physics may be non-minimal, and the most striking experimental discoveries may not have any obvious connection to the "big questions." It is therefore important to look for any new physics that can manifest itself by the enhanced energy reach of a new accelerator, especially if it arises from a simple extension of the standard model. This is especially important at a hadron collider such as the LHC, where large backgrounds mean that finding a signal often requires knowing what to look for.

The classic example of simple new physics not directly motivated by electroweak symmetry breaking is a Z'. This involves extending the standard model with a $U(1)'$ gauge group, plus a new Higgs sector that breaks the $U(1)'$ symmetry. The only parameter of the new Higgs sector relevant for phenomenology is the Z' mass, so the only parameters in the model are the $U(1)'$ coupling g' and $m_{Z'}$. In addition, there is a discrete choice of the charges of standard model fields under $U(1)'$. (We assume that some of these charges are nonzero, otherwise the quirks are not observable.) Although the Z' mass is not directly tied to electroweak symmetry breaking, the focus is on the phenomenologically interesting regime (very roughly $m_{Z'} \sim$ TeV) that is not excluded by existing experiments, but may be probed at LHC.

In this paper, we consider another equally minimal extension of the standard model. We assume that there is an additional unbroken $SU(N)$ gauge group with some fermions Q, $\bar{Q}$ in the fundamental representation. (The qualitative features of the model are unchanged if the particles are scalars rather than fermions.) This model is parameterized by the mass of the new particles m_Q and the $SU(N)$ gauge coupling, which can be parameterized by the scale Λ where it gets strong. In addition, there is a discrete choice of the standard model gauge quantum numbers of the new fermions. (We assume that some of these charges are nonzero, otherwise the Z' is not observable.) We assume that the mass of the fermions is in the phenomenologically interesting range (very roughly 100 GeV $\lesssim m_Q \lesssim$ TeV) that is not excluded by existing experiments, but may be probed at LHC.

New strong interactions have been considered often in particle physics, usually with strong interaction scales at or above a TeV. We instead consider the case where

$\Lambda \ll$ TeV, in particular

$$\Lambda \ll m_Q. \tag{1.1}$$

We therefore refer to the new gauge interaction as "infracolor." Note that if Q is the lightest particle in the fundamental representation of infracolor then it is automatically stable, since there is no lighter state with the same quantum numbers. We have learned recently that this model was first considered by L. B. Okun [1], who called the new particles "thetons." This model was considered as a limit of QCD in Ref. [2]. Ref. [3] also mentioned this model as an example of a "hidden valley" model.

This paper will consider the phenomenology of these models with values of Λ ranging over many orders of magnitude (roughly 100 eV to 100 GeV). All these values are natural, since Λ is related to the fundamental gauge coupling g_0 defined at a scale μ_0 by

$$\Lambda = \mu_0 \, e^{-8\pi^2/b g_0^2}, \tag{1.2}$$

where b is the 1-loop coefficient of the $SU(N)$ gauge coupling beta function. The scale Λ is exponentially sensitive to the value of g_0^2, so each decade of energy is roughly equally likely.

Cosmology places strong constraints on new light physics, even if it is weakly coupled to the standard model. However, if the reheat temperature is sufficiently low ($T \lesssim$ GeV) the infracolor sector is never in thermal equilibrium, and there are no cosmological consequences. This shows that there are no model-independent constraints from cosmology on this physics. If we assume thermal abundances for the new particles the cosmology is complicated, but may also be viable [4].

This paper will focus on the collider phenomenology of this model at the qualitative level. This phenomenology of this simple model is surprisingly exotic. The reason is that breaking of the infracolor gauge string is exponentially suppressed due to the large Q mass. As we will see, this leads to very exotic phenomenology, so we call the new particles "quirks."[1]

The collider phenomenology of quirks depends crucially on the length of the strings. This is set by the scale where the quirk kinetic energy is converted to string potential energy. Since the typical event is not close to threshold, it has kinetic energy $\sim m_Q$ and gives a string length scale

$$L \sim \frac{m_Q}{\Lambda^2} \sim 10 \text{ m} \left(\frac{m_Q}{\text{TeV}}\right) \left(\frac{\Lambda}{100 \text{ eV}}\right)^{-2}. \tag{1.3}$$

[1] This can also be motivated by the replacements "strong" $\rightarrow$ "string", "quark" $\rightarrow$ "quirk".

We will consider collider signals for string length scales ranging from the size of detectors (~ 10 m) to microscopic scales.

This paper is organized as follows. In Section 2, we briefly discuss model-building issues such as naturalness and unification, as well as indirect constraints from precision electroweak data, cosmology, and astrophysics. In Section 3 we discuss production of quirks and strings. In Section 4 we discuss signals for macroscopic strings. In Section 5 we consider annihilation of quirks catalyzed by the string. In Section 6 we discuss the signals of mesoscopic strings, those that are too small to be resolved in a detector but large compared to atomic scales. In Section 7 we discuss the collider signals from microscopic strings. Section 8 contains our conclusions.

2 Models and Indirect Constraints

In this section, we discuss model-building issues such as naturalness and unification, as well as indirect constraints from precision electroweak constraints and cosmology. This discussion is fairly standard, and our conclusion is that there are no strong model-independent constraints on quirks from these considerations.

2.1 Coupling to the Infracolor Sector

Because we assume that the scale of infracolor strong interactions is below the weak scale, the hadrons of the infracolor sector are kinematically accessible to existing experiments. However, the standard model is uncharged under infracolor, and therefore a quirk loop is required to couple the sectors. Since the quirks are heavy, this leads to highly suppressed couplings to the infracolor sector.

The leading coupling between the standard model and the infracolor sector at low energies arises from the diagram of Fig. 1a. This gives rise to the dimension-8 effective operator

$$\mathcal{L}_{\text{eff}} \sim \frac{g^2 g'^2}{16\pi^2 m_Q^4} F_{\mu\nu}^2 F_{\rho\sigma}'^2. \tag{2.1}$$

The 2-loop diagram of Fig 1b can couple the infracolor gauge fields to dimension-3 fermion bilinears, but these have an additional helicity suppression in addition to the additional loop suppression, and are therefore suppressed. For $m_Q \gtrsim 100$ GeV this operator is far weaker than the weak interactions, so production of infracolor gauge bosons at colliders with energy below the quirk mass is completely negligible. Probing this sector at colliders requires sufficient energy to produce quirks directly.

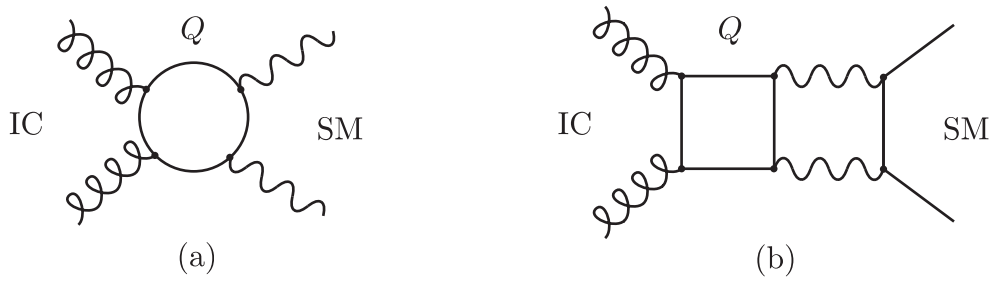

Fig. 1. Loop graphs contributing to the coupling of the standard model and infracolor sector.

The operator Eq. (2.1) mediates infracolor glueball decay, for example to photons or gluons. The rate is of order

$$\Gamma \sim \frac{1}{8\pi}\left(\frac{g^2 g'^2}{16\pi^2 m_Q^4}\right)^2 \Lambda^9. \tag{2.2}$$

Note that this is very sensitive to both Λ and m_Q. We have

$$c\tau \sim 10 \text{ m } \left(\frac{\Lambda}{50 \text{ GeV}}\right)^{-9}\left(\frac{m_Q}{\text{TeV}}\right)^{-8}. \tag{2.3}$$

We see that the infracolor glueballs can decay inside a particle detector for $\Lambda \gtrsim 50$ GeV, while the lifetime becomes longer than the age of the universe for $\Lambda \lesssim 50$ MeV.

2.2 Star Cooling

Stars with temperature $T \gtrsim \Lambda$ can potentially cool due to emission of infracolor glueballs. Due to the rapid decoupling of infracolor interactions from standard model interactions in Eq. (2.1), we find that this does not give interesting bounds.

We will focus on bounds from SN1987A, which has the highest temperature ($T \sim 30$ MeV) of the astrophysical systems used to constrain light particles. We can estimate the bounds by comparing to axion cooling, which constrains the axion decay constant $f_a \gtrsim 10^9$ GeV. For both the axion and infracolor, the dominant energy loss mechanism is nuclear bremmstrahlung.

Below the QCD scale the coupling Eq. (2.1) gives rise to an effective coupling of infracolor gauge fields to nucleons:

$$\mathcal{L}_{\text{eff}} \sim \frac{g^2 g'^2 \Lambda_{\text{QCD}}}{16\pi^2 m_Q^4}\bar{N}NF'^2_{\mu\nu}. \tag{2.4}$$

Here $\Lambda_{\rm QCD} \sim 1$ GeV is the scale of strong QCD interactions. Factors of 4π have been put in using "naïve dimensional analysis" [5]. This is to be compared with the axion coupling

$$\mathcal{L}_{\rm eff} \sim \frac{\Lambda_{\rm QCD}}{f_a} a \bar{N} N. \tag{2.5}$$

We therefore have

$$\frac{\text{rate of infracolor production}}{\text{rate of axion production}} \sim \left(\frac{g^2 g'^2 \Lambda_{\rm QCD}}{16\pi^2 m_Q^4}\right)^2 T^6 \Big/ \frac{\Lambda_{\rm QCD}^2}{f_a^2}, \tag{2.6}$$

which gives a bound of $m_Q \gtrsim 10$ GeV. Although these estimates are very crude, the fact that the infracolor emission falls as $1/m_Q^8$ means that the rate is highly suppressed in the interesting regime $m_Q \gtrsim 100$ GeV.

2.3 Cosmology

If the infracolor gauge interactions and/or the quirks have thermal abundances early in the universe, there are stringent cosmological constraints. This paper will focus mainly on collider physics, so we make only some simple remarks here, leaving a more complete investigation to future work.

The rapid decoupling of the infracolor interactions means that infracolor glueballs are not produced if the reheating temperature is sufficiently low. Assuming $T_{\rm RH} \gg \Lambda$, the condition for infracolor interactions to be out of equilibrium is

$$\Gamma \sim \left(\frac{g^2 g'^2}{16\pi^2 m_Q^4}\right)^2 T_{\rm RH}^9 \gtrsim \frac{T_{\rm RH}^2}{M_{\rm P}}, \tag{2.7}$$

which is satisfied for $T_{\rm RH} \lesssim$ GeV. This is easily sufficient for nucleosynthesis at $T \sim$ MeV, the highest temperature about which we have secure cosmological knowledge.

This is not an entirely satisfactory solution to cosmology, since it requires dark matter and the baryon asymmetry to be produced at low termperatures. This is possible with *e.g.* MeV dark matter [6] and low-scale baryogensis [7]. We can avoid exotic low-temperature cosmology by having quirks decay to infracolored states that are sterile under the standard model. These decays can have lifetimes long compared to collider time scales, but short enough to avoid cosmological constraints. We will not discuss the details here. For the present discussion it is sufficient that low reheat temperatures are not in conflict with nucleosynthesis, so there is no model-independent constraint from cosmology.

2.4 Precision Electroweak Data

Precision electroweak data constrains new physics at the TeV scale. However, if the quirks are in a vector-like representation of the standard model gauge group they can have a TeV mass term that does not break electroweak symmetry. Furthermore, virtual quirks are necessarily created in pairs, so there are no tree-level effects on electroweak observables. There is therefore no constraint on such models from precision electroweak data.

2.5 Model Building

Next we discuss the plausibility of this kind of new physics. The existence of additional gauge groups with matter in bifundamental representations is a hallmark of brane constructions in string theory. As we will see the most natural quirk sector is vectorlike, which means that it requires no additional projections of the kind needed to obtain a chiral theory such as the standard model. A quirk/infracolor sector can therefore arise simply and naturally from string theory.

In fact, in realistic supersymmetric theories there is already at least one set of vectorlike fields, namely the Higgs bosons. These must have a supersymmetric "μ term" at the weak scale, otherwise we have either light Higgsinos or no electroweak symmetry breaking. Any mechanism that generates the μ term can also generate a weak-scale mass for the quirks. This means that no additional assumptions are required to explain the origin of the quirk mass in supersymmetric theories. It is also trivial to preserve gauge coupling unification in supersymmetric theories by assuming that the quirks come in complete GUT representations. The simplest example is that the quirks are in a

$$\mathbf{5} \oplus \bar{\mathbf{5}} \to (\mathbf{3}, \mathbf{1})_{\frac{1}{3}} \oplus (\bar{\mathbf{3}}, \mathbf{1})_{-\frac{1}{3}} \oplus (\mathbf{1}, \mathbf{2})_{\frac{1}{2}} \oplus (\mathbf{1}, \mathbf{2})_{-\frac{1}{2}}. \tag{2.8}$$

In this model there is no tree-level Yukawa interaction that can split the masses of the doublet. These splittings will arise from loop graphs, and will be very small. There is also no tree-level interaction that allows either the color triplet or the electroweak doublet to decay to the other, so this model naturally has both colored and uncolored quirks.

In fact, a quirk/infracolor sectors have already appeared in some model-building motivated by the hierarchy problem. Such a sector was proposed in Ref. [8] to give additional loop contributions to the physical Higgs mass in supersymmetry. Scalar quirks ("squirks") appear in models of "folded supersymmetry" [9].

Small values of Λ are perfectly compatible with grand unification. As an example, we consider the MSSM with an $SU(2)$ infracolor gauge group, with quirks in the $\mathbf{5} \oplus \bar{\mathbf{5}}$ representation (see Eq. (2.8)). The infracolor beta function is equal to the color beta function at one loop, simple unification implies that the infracolor gauge coupling is equal to the QCD gauge coupling at the scale of superpartner masses. The scale of infracolor interactions is then of order 100 MeV. If the theory above the TeV scale has respectively 1, 2, 3 additional pairs of infracolor fundamentals, the infracolor scale is respectively MeV, 10 keV, 100 eV.

3 Quirk Production and String Formation

3.1 Absence of String Breaking

The reason that infracolor gauge strings do not break was already discussed in the introduction. A virtual quirk-antiquirk pair costs energy at least $2m_Q$, and will have a typical separation of order m_Q^{-1}. This lowers the string potential energy only by an amount of order $\Lambda^2/m_Q \ll 2m_Q$, so this process cannot go on shell (see Fig. 2). An on-shell transition requires eliminating a length of string of order $\Delta L \sim m_Q/\Lambda^2 \gg \Lambda^{-1}$. The rate for this transition will be exponentially suppressed.

This transition is closely analogous to the Schwinger mechanism of pair creation of charged particles by a weak electric field [10]. For charged particles with $m \gg E^{1/2}$, the rate for pair creation is

$$\Gamma/V = \frac{E^2}{4\pi^3} e^{-\pi m^2/E}. \tag{3.1}$$

Modeling a gauge string as a flux tube with area A and color electric field E, the string tension is $\sigma \sim E^2 A$, so we have

$$\Gamma/L \sim \frac{\sigma}{4\pi^3} e^{-\pi m_Q^2/E}. \tag{3.2}$$

For a string of length $L \sim m_Q/\sigma$, we estimate $E \sim \pi\Lambda^2$ and obtain a lifetime

$$\tau \sim \frac{4\pi^3}{m_Q} e^{m_Q^2/\Lambda^2}. \tag{3.3}$$

For $\Lambda/m_Q \lesssim 10^{-1}$ this is already longer than the age of the universe for $m_Q \gtrsim 100$ GeV.

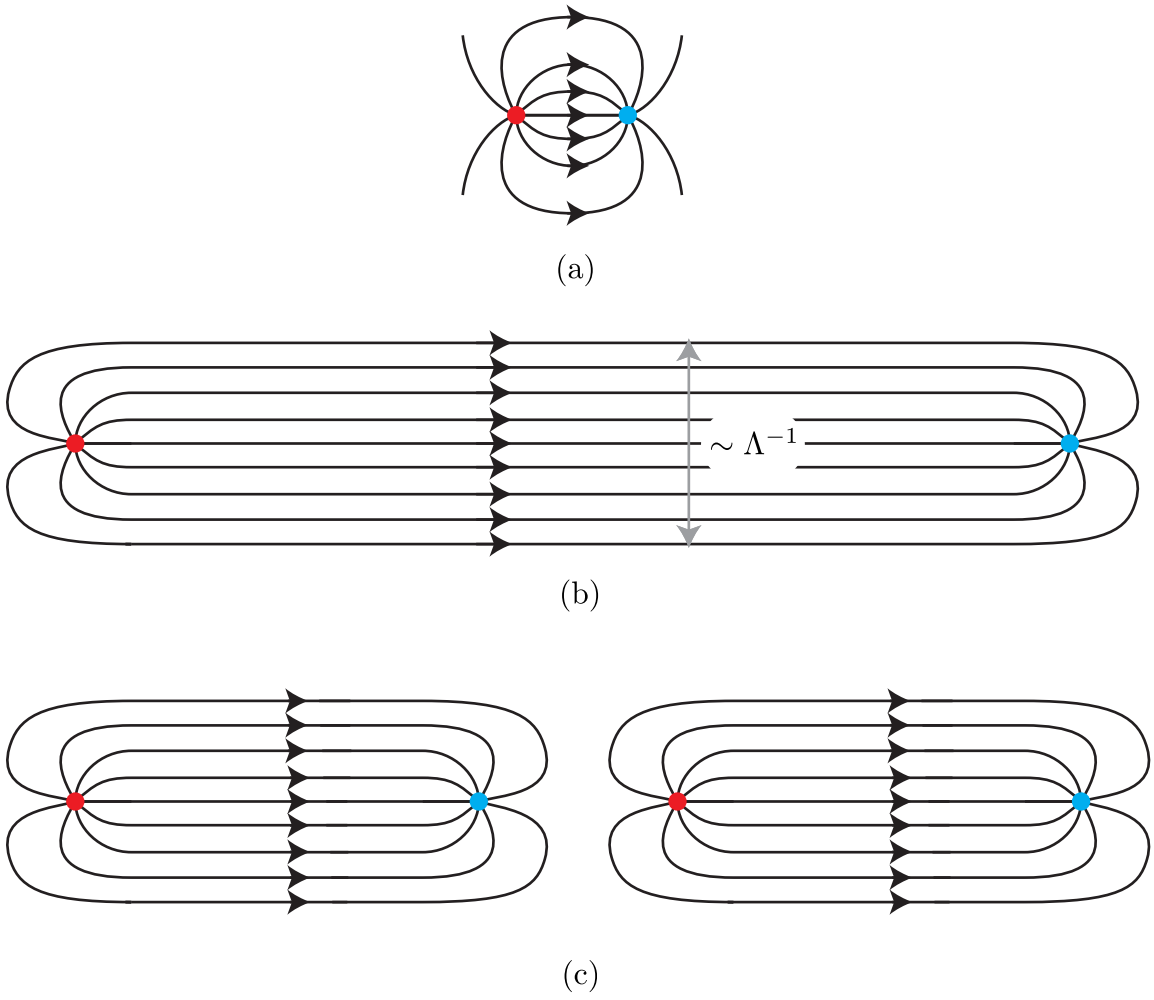

Fig. 2. Schematic view of color flux for quirk separation for (a) $r \ll \Lambda^{-1}$ and (b) $r \gg \Lambda^{-1}$. String breaking (c) requires a quirk-antiquirk pair to be created, which costs energy $2m_Q \gg \Lambda$.

3.2 Quirk Production

Quirk production involves energy and momentum transfer of order $m_Q \gg \Lambda$ and $\Lambda_{\rm QCD}$, and is therefore a hard perturbative process. The total cross section for quirk production at Tevatron and LHC at leading order in perturbation theory are shown in Fig. 3. This does not include Sommerfeld enhancement due to attractive infracolor and/or QCD interactions [11]. This will increase the cross section near threshold, and need to be included in a more detailed study. The Coulomb interactions are familiar,

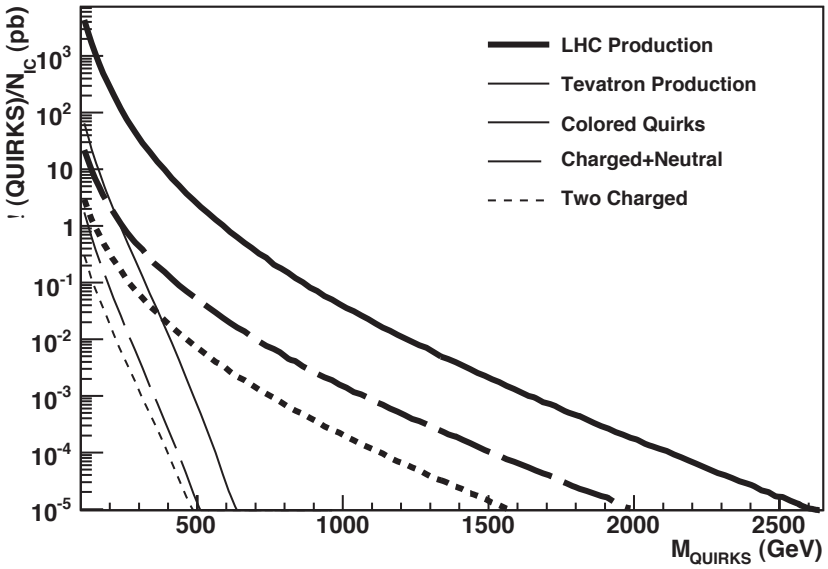

Fig. 3. Quirk production cross section at the Tevatron and LHC.

so we consider briefly the Sommerfeld enhancement due to the long-range infracolor interactions. These become relevant only when the string length is longer than Λ^{-1}, which requires $\beta \gtrsim (\Lambda/m_Q)^{1/2}$. The linear potential will be a large perturbation on the state if the potential energy changes significantly in one de Broglie wavelength. We therefore compute the ratio of this change to the kinetic energy:

$$\frac{\Delta V}{K} \sim \frac{\Lambda^2/m_Q\beta}{m_Q\beta^2} \sim \frac{\Lambda^2}{m_Q^2}\,\frac{1}{\beta^3} \lesssim \left(\frac{\Lambda}{m_Q}\right)^{1/2}. \tag{3.4}$$

We see that the effects of the long-range potential are always small enough to be treated as a perturbation, although they may be numerically significant for the largest values of Λ.

Returning to Fig. 3, we conclude that the cross sections are substantial up to several TeV for LHC. (Note that the cross section is proportional to $N_{\rm IC}$.) Many quirk signatures are completely background-free (as we will see), so even a few reconstructed events may be sufficient for discovery.

3.3 String Formation

The effect of non-perturbative infracolor interactions and the formation of an infracolor string has many points in common with hadronization of heavy stable quarks in QCD, so we review this first.

Imagine that there is a heavy ($m \gg \Lambda_{\rm QCD}$) stable quark (or squark or gluino) in QCD in addition to the light quarks. Below the free quark threshold at $2m$ these can be produced in a Coulomb-like bound state (quarkonium). Formation of such a low-lying bound state requires that the quirk pair be produced just below the free threshold, *i.e.* $2m - E \sim \alpha_3^2(m)m$. Wavefunction overlap factors give a suppression of the rate by additional powers of $\alpha_3(m)$, and so the rate for the production of these bound states is much smaller than the production rate for unbound quarks. The quark production cross section is dominated by quarks with kinetic energy $K = E - 2m \sim m \gg \Lambda$. In this regime, threshold effects are unimportant and the production process is perturbatively calculable in an expansion in $\alpha_3(m)$.

We now consider the hadronization of heavy stable quarks with $K \sim m$. Kinematically, it is possible that a large fraction of the kinetic energy is converted to light hadrons, resulting in a jet surrounding the heavy quarks. However, because the quark is very heavy its kinetic energy cannot be efficiently converted into production of light hadrons. The basic reason is that the strong interactions have a range of order $\Lambda_{\rm QCD}^{-1}$, so once the heavy quarks are separated by a distance $r \gg \Lambda_{\rm QCD}^{-1}$ the strong interactions become perturbative. It is traditional in heavy quark physics to refer to the non-perturbative QCD interactions as "brown muck" to emphasize how little we know about it. The size of the force exerted by the brown muck is of order $\Lambda_{\rm QCD}^2$, so the total energy transfered from quark kinetic energy into light hadrons is only of order

$$\Delta E \sim F \Delta r \sim \Lambda_{\rm QCD}. \tag{3.5}$$

There is a tail at large ΔE that can be described in perturbative QCD by additional hard gluons.

We now turn to quirks. The infracolor interactions effectively have infinite range because of the infracolor string, and we might worry that the conversion of quirk kinetic energy to infracolor hadrons (glueballs) never stops. We consider events far from threshold ($K \sim m_Q$), for which the string length $L \sim m_Q/\Lambda^2 \gg \Lambda^{-1}$, long enough to be a well-defined object. In this case the string rapidly straightens out, approaching a configuration close to its local ground state.

To understand this, it is helpful to restate in a somewhat formal way the obvious fact that well-separated QCD hadrons from heavy stable quark production do not

continue to lose energy to hadron emission. The point is that a state consisting of well-separated hadrons is locally (on scales of order $\Lambda_{\rm QCD}$) a boost of the ground state. Let us apply this point of view to a rapidly-stretching infracolor string with heavy quirks at the ends. In the center of mass frame, the middle of the string has zero transverse velocity. A long QCD string is described by the Nambu-Goto action (see below), which has no longitudinal excitations. This string configuration is therefore identical to the ground state in the center of mass frame. Near the ends of the string, only the acceleration of the ends represents a departure from a boost of a ground state. The acceleration is given by

$$a = \frac{F_{\rm string}}{m_Q} \sim \frac{\Lambda^2}{m_Q} \ll \Lambda. \tag{3.6}$$

Because the acceleration is very small on the scale Λ, there is no energy loss to infracolor radiation from the ends. The infracolor strings can be thought of as being close to the static limit $m_Q \to \infty$. This is qualitatively different from the open strings of string theory, which have massless ends.

The non-perturbative infracolor "brown muck" is therefore effective in radiating glueballs only when the quirk separation is of order Λ^{-1} or less. Similarly to the case of heavy stable quark production in QCD, this results in an energy of order Λ being radiated into infracolor glueballs during the production process.

3.4 Dynamics of Quirks and Strings

We now discuss the motion of the quirk-string system produced as described above. As long as we are considering excitations of the string with wavelengths long compared to Λ^{-1}, we can use an effective description in which the string is elementary. This is analogous to the chiral Lagrangian describing pion interactions for energies small compared to $\Lambda_{\rm QCD} \sim$ GeV.

Gauge strings are described at long distances by the Nambu-Goto action. This is not *a priori* obvious, since there are other universality classes of strings that break additional Lorentz symmetry. For a clear discussion of this point, see Ref. [12]. Strong numerical evidence that the long-wavelength fluctuations of the QCD string are described by the Nambu-Goto action was obtained in Ref. [13].

The action for a pair of heavy quarks connected by a gauge string can be written

$$S = -m_Q \sum_{i=1}^{2} \int d\tau_i - \sigma \int dA + S_{\rm ext}, \tag{3.7}$$

where $d\tau_i$ is the proper length of the worldline for quirk i, dA is the proper area element of the string worldsheet, and $S_{\rm ext}$ represents the effect of external forces.

Fig. 4. Definitions used in quirk equations of motion.

Here $\sigma \sim \Lambda^2$ is the string tension. In the variation with respect to the quirk position, there is a surface term from the string action that generates the string force on the quirks. We therefore obtain the quirk equation of motion

$$\frac{\partial}{\partial t}\left(m\gamma\vec{v}\right) = -\sigma\left[\sqrt{1-\vec{v}_\perp^{\,2}}\,\hat{s} + \frac{v_\parallel}{\sqrt{1-\vec{v}_\perp^{\,2}}}\,\vec{v}_\perp\right] + \vec{F}_{\rm ext}, \tag{3.8}$$

where $\vec{v}$ is the quirk velocity, and $\vec{v}_\parallel$ and $\vec{v}_\perp$ are the components of the quirk velocity parallel and perpendicular to the string:

$$\vec{v}_\parallel = (\vec{v}\cdot\hat{s})\hat{s}, \qquad \vec{v}_\perp = \vec{v} - \vec{v}_\parallel, \tag{3.9}$$

where $\hat{s}$ is a unit vector along the string pointing outward at the endpoints (see Fig. 4). The second term in brackets is similar to a Lorentz force, and is required by relativistic invariance.

The gauge string is a dynamical object with its own complicated equation of motion. However, if the quirks have no further interactions after they are produced (*e.g.* with matter in the detector) then in the center of mass frame the string remains straight. Therefore, the only long-wavelength excitations of the string arise from quirk interactions with matter. If the string force is much larger than matter forces

$$F_{\rm ext} \ll \Lambda^2, \tag{3.10}$$

then we expect that the string will remain approximately straight in the center of mass frame. The maximum force from either ionization or nuclear energy loss is of order $(100\text{ eV})^2$, so the straight-string approximation is guaranteed to hold only for $\Lambda \gg 100$ eV. Note that this translates to $L \ll 10$ m, so all but the longest strings of interest in colliders can be approximated as straight. The full string dynamics is sufficiently complicated that it would be useful to check this by direct simulation.

A potential concern is that interactions of the quirks with matter involve collisions with momentum transfer that may be larger than Λ. For relativistic quirks, the energy

and momentum transfer in these processes is of order

$$\begin{aligned} \Delta p_{\rm ion} &\sim m_e \sim \text{MeV}, \\ \Delta p_{\rm nuc} &\sim \Lambda_{\rm QCD} \sim \text{GeV}. \end{aligned} \tag{3.11}$$

We now ask whether this leads to the emission of infracolor glueballs. The important point is that only the quirk has electromagnetic or QCD interactions, so this energy and momentum transfer is to the quirk, not the infracolor string, which is sterile under the standard model. The change in the quirk velocity is of order

$$\Delta v \sim \frac{\Delta p}{m_Q} \ll 1. \tag{3.12}$$

This is a small perturbation as seen by the infracolor interactions, and does not lead to the emission of an infracolor glueball. This is very clear if we consider a heavy stable quark, which is surrounded by QCD brown muck, but has no string attached. In this case, the perturbation is equivalent to the quark remaining at rest while the brown muck gets a velocity Δv in the opposite direction. This transfers energy $\Lambda_{\rm QCD}\Delta v^2 \ll \Lambda_{\rm QCD}$ to the brown muck. If this energy is smaller than the mass of the lightest hadron that can be emitted (a pion in this case), there is no transition and the process is elastic. For quirks, the total mass of a long string may be much larger than Λ, but glueball emission is a local process with a scale set by Λ^{-1}. We therefore expect hadron emission to be suppressed as in the QCD case.

4 Macroscopic Strings

We now consider strings with lengths longer than the tracking resolution of a typical detector, very roughly $L \gtrsim$ mm. In this case, the quirk and the antiquirk appear as separated particles connected by a string. Strings much longer than a detector size will not have observable effects on the quirk trajectories, so we are considering mm $\lesssim L \lesssim 10$ m corresponding to

$$100 \text{ eV} \lesssim \Lambda \lesssim 10 \text{ keV} \tag{4.1}$$

for $m_Q \sim$ TeV.

4.1 Anomalous Tracks

One obvious signature in this case is the anomalous quirk tracks in the case where one or both quirks are electrically charged. Because the string tends to accelerate the

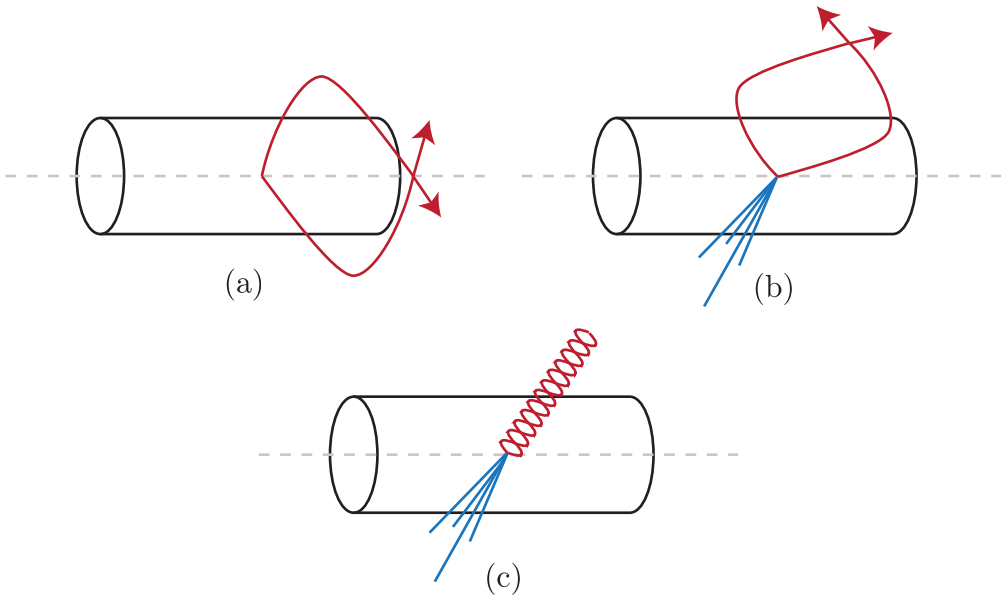

Fig. 5. Anomalous tracks from quirks with macroscopic strings.

quirks toward each other, we can have events such as those depicted schematically in Fig. 5. In these events, the curvature of the tracks is qualitatively different from the curved track of a particle in the magnetic field of the detector. For example, a magnetic field along the beam direction curves tracks only in the r-ϕ plane, while quirk tracks generally have curvature in the r-z plane. Therefore, unambiguous observation of only a single event of this type is sufficient for discovery of macroscopic strings!

Do quirks annihilate when the string force brings them back together? For the case of macroscopic strings considered here, this is highly suppressed by the fact that annihilation requires the quirk to be in a state of relative angular momentum $\ell \sim 1$, while interactions with matter change the angular momentum by much larger amounts due to the long lever arm. Even a single ionization interaction gives

$$\Delta\ell \sim \Delta p L \sim m_e \frac{\Lambda^2}{m_Q} \sim \left(\frac{m_Q}{\text{TeV}}\right)\left(\frac{\Lambda}{\text{GeV}}\right)^{-2}. \tag{4.2}$$

The infracolor "brown muck" surrounding the quirk has a much larger cross section of order Λ^{-2}, and can therefore interact for angular momenta $\ell \lesssim m_Q/\Lambda$. A single ionization interaction changes the angular momentum more than this for $\Lambda \lesssim$ MeV. We conclude that quirks with macroscopic strings do not annihilate.

The difficulty in detecting quirks with macroscopic strings is that triggers and

track reconstruction algorithms are designed for conventional tracks, and will likely miss these events altogether. Defining an efficient trigger for these events that has low background from standard physics and instrumental noise is worth further investigation. A simpler strategy is to focus on events where the quirk pair is produced in association with one or more hard jets or photons (see Fig. 5b and 5c). Standard reconstruction algorithms will fail to reconstruct the quirk tracks, resulting in missing p_T balanced by jets or photons. If such events are discovered, careful examination of the signal events in the missing p_T direction can reveal the presence of "quirky" tracks.

4.2 Stopping Quirks

Do quirks stop in the detector? The stopping of heavy stable charged and/or strongly-interacting particles has been extensively studied [14], with the conclusion that typically a significant fraction do indeed stop inside the detector. For quirks there is an additional complication from the string interaction. In order for quirks to come to rest, they must become bound to the lattice in the detector material. If the string force is stronger than the forces that bind the quirks to the lattice, they will continue to be dragged by the string.

We first consider possible final states of quirks bound to the lattice. The binding mechanism depends on the standard model quantum numbers of the quirks. If quirks are electrically charged but uncolored, they can be electronically bound to the lattice similarly to ordinary nuclei. This is particularly clear for positively charged quirks, which can share a lattice site with an ordinary nucleus since there is no constraint from the exclusion principle. Negatively charged quirks will experience an electrical potential with opposite sign, and it is reasonable to assume that they will also find a stable local minimum. If quirks are colored, they will form quirk hadrons whose charge may change with time because of inelastic strong interactions that change the valence quark structure. We expect quirk hadrons to bind efficiently with nuclei, and these can also become stuck in the lattice.

In all of these cases, the binding energy of the quirk (or quirk-nucleus bound state) to the lattice is of order eV, and the typical size of a potential well is of order Å. (The binding energy is set by the electron mass, and is independent of the mass of the heavy particle. For example, the binding energies for heavy and light nuclei are all several eV.) Therefore, the force required to remove a bound quirk from the lattice is of order

$$F_{\rm latt} \sim \frac{\rm eV}{\rm \AA} \sim (100\ {\rm eV})^2. \tag{4.3}$$

If the string force is larger than this, the lattice cannot bind the quirk and it will not stop.

Even if $\Lambda \ll 100$ eV, the string force gives the quirks substantial kinetic energy, making it more unlikely for them to bind to the lattice. The binding energy of a nucleus in the lattice is of order eV, and it is reasonable to assume that the lattice cannot absorb energy larger than this without breaking. Therefore, a quirk nucleus will not bind with the lattice if its kinetic energy is large compared to eV. This requires

$$\beta \lesssim 10^{-6} \left(\frac{m_Q}{\text{TeV}}\right)^{1/2}. \tag{4.4}$$

For such small values of β ionization forces are described by the theory of Fermi and Teller [15], extended by Lindhard [16]. We have

$$F_{\text{ion}} \sim \Lambda_0^2 \beta, \qquad \Lambda_0 \sim \text{keV}. \tag{4.5}$$

The ionization force for different nuclei in the same material vary over about an order of magnitude, suggesting an uncertainty of an order of magnitude in Λ_0. Balancing this against the string force gives a terminal speed

$$\beta_* \sim \left(\frac{\Lambda}{\text{keV}}\right)^2. \tag{4.6}$$

Imposing Eq. (4.4) then gives

$$\Lambda \lesssim \text{eV} \left(\frac{m_Q}{\text{TeV}}\right)^{1/4}. \tag{4.7}$$

This bound is proportional to Λ_0, so there is an uncertainty of an order of magnitude in this estimate. Despite this uncertainty, it seems unlikely that quirks stop in the detector even for the smallest values of Λ of interest.

If one quirk stops in the detector, the other will eventually lose its kinetic energy and annihilate with it. If both quirks stop, there is a string stretched between them. This string can interact with strings of subsequently produced quirks, producing even more bizarre events. One can also imagine releasing such quirks by *e.g.* melting the material in which they are trapped, and looking for the subsequent annihilation. These are amusing possibilities that might be worth taking seriously if more a detailed study indicates that large numbers of quirks in fact stop in the detector.

4.3 Quirk Annihilation

Although the string force tends to prevent the quirks from stopping, it also tends to bring them together to allow them to annihilate. In particular, sufficiently slow

charged quirks (or quirk nuclei) will reach the terminal speed given by Eq. (4.6). The subsequent motion of the quirks is damped, so these quirks can find each other more efficiently. Of course, this mechanism only works if both quirks are electrically charged.

The linear form of the damping force holds up to velocities of order α. For such small velocities slow-moving colored quirks can bind with nuclei, making them effectively charged and subject to the mechanism considered here. The maximum ionization force is of order $(100\text{ eV})^2$, so this mechanism only works for $\Lambda \lesssim 100$ eV. Ionization energy loss is a good description as long as the separation of the quirks is larger than atomic distances of order Å. Even for distances smaller than Åthe energy loss is more complicated, but we expect charged quirks to exchange energy efficiently with electrons. We therefore assume that they annihilate on a time scale relevant for collider searches.

An interesting question is the distribution of annihilation events in the detector. We have made a crude simulation of this using the straight string approximation. We include ionization energy loss as a continuous force, approximating the detector as solid iron. We also include a crude approximation to nuclear energy loss, although that does not really affect our results. We assume that all quirks that reach terminal speed and come close together in the detector annihilate sufficiently rapidly to be seen. An example of our results are shown in Fig. 6. Note that most of the annihilations take place near the beam. This is easy to understand. Most of the events where both quirks become damped arise from events where quirks are produced nearly back-to-back in the central region of the detector. In such events the quirks will have speed less than α at the turning points, and therefore they become damped there. Their subsequent motion is essentially constant velocity toward each other, and they meet near the beam axis.

The distribution of annihilation events is very different that of late-decaying particles stopped in the detector [14]. More realistic simulations should be done to check the distribution of these events. Another difference is that most examples of late-decaying particles that have been discussed in the literature decay partly to missing energy while quirks will annihilate to visible energy in most modes.

Another aspect of quirk annihilation that can in principle give a signal is the ionization track of the damped quirks before they re-annihilate. The ionization is large compared to typical particles, but the track is very slow ($\beta \lesssim \alpha$). Presumably, it will therefore generate "stub" tracks in many events that are triggered for other reasons, and these stubs can in principle be connected. Since these tracks lead to annihilation events (assuming that the timescale for energy loss is sufficiently short)

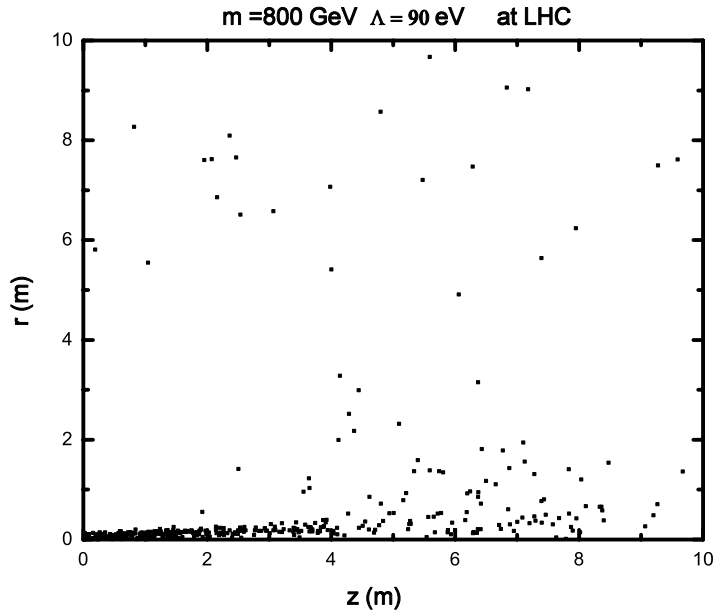

Fig. 6. Results from a crude simulation of position of quirk annihilation events relative to collision point.

so one can start looking for them there.

The previous discussion assumes that both quirks are electrically charged, so that they both experience ionization forces. If the quirks are colored, their charge state may change on a distance scale given by the nuclear mean free path (~ 10 cm in iron) complicating the phenomenology further. One other case that bears mentioning is the case of uncolored quirks where one is charged and the other is neutral, *e.g.* produced by s-channel W exchange. In this case, the charged quirk can become damped, while the neutral quirk will not interact with matter. In this case, the charged quirk will be driven by the invisible neutral quirk which can have a much larger amplitude of motion. This can result in truly bizarre charged tracks such as the one illustrated in Fig. 7. Since the damped quirk is moving very slowly ($\beta \lesssim \alpha$) these events will be very difficult to detect.

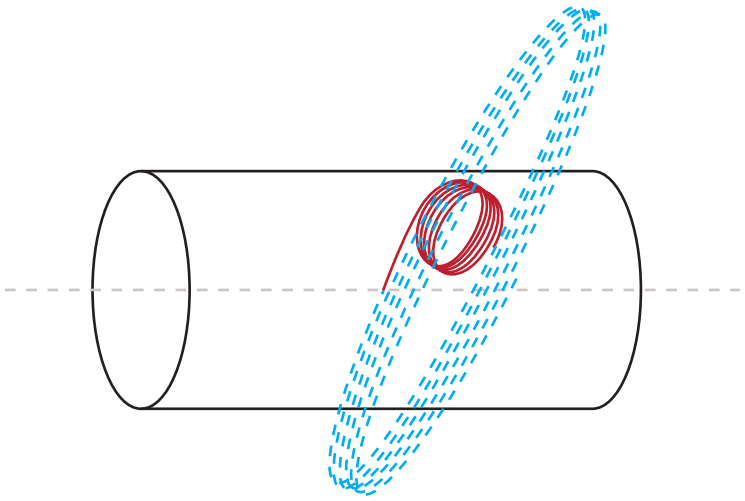

Fig. 7. Highly exotic track resulting from an electrically charged quirk (solid track) becoming damped in the detector, while its neutral partner (dashed track) drives its motion. The neutral track will be unobservable.

5 Prompt annihilation

We now consider in more detail the question of quirk annihilation, which is very important for the phenomenology of microscopic strings. The momentum transfer in the annihilation process is of order m_Q, which means that the quirks must come within a distance of order m_Q^{-1} in order to annihilate. Equivalently, the cross section is dominated by partial waves with relative angular momentum $\ell \lesssim p/m_Q \lesssim 1$. Because the maximum quirk separation L is much larger than the microscopic scales m_Q^{-1} and $\Lambda_{\rm QCD}^{-1}$, there is a large lever arm with which interactions with matter can change the angular momentum. However, if the string is sufficiently short matter effects are not important (we will be more precise about this below). In this section we analyze annihilation of quirks in the absence of matter effects.

A crucial question is the rate of transfer of energy and angular momentum from the bound state. An important feature is interactions of the non-perturbative "brown muck" surrounding the quirks, from infracolor and/or QCD interactions. The cross section for these interactions is much larger than the hard annihilation of quirks, and may change the energy and angular momentum of the system, thereby suppressing annihilation. We also consider the effects of radiation as a mechanism of losing

energy and angular momentum, and we argue that this is generally unimportant as a mechanism of energy loss.

5.1 Quirkonium

Quirk pairs produced near threshold can form a Coulomb-like "quirkonium" bound state. Formation of such a low-lying bound state requires that the quirk pair be produced near threshold, *i.e.* $|E - 2m_Q| \lesssim \alpha^2 m_Q$, where α is the infracolor gauge coupling, or the QCD gauge coupling if the quirks are colored and $\Lambda < \Lambda_{\rm QCD}$. These bound states will annihilate promptly into pairs of gluons or quarks (for colorful quirks). This signal has been considered for stable gluinos in Ref. [17] where it was found to be less sensitive than searches for unbound gluinos. We expect the result for quirks to be qualitatively similar, in that signals for highly excited quirks ($E - 2m_Q \gg \alpha^2 m_Q$) will be more sensitive.

5.2 Highly Excited Bound States

We are interested in the majority of events that produce quirks that are not close to threshold, *i.e.* $E - 2m_Q \sim m_Q$. As discussed in Section 3 quirk production is essentially perturbative, so quirk pairs are produced in a state of relative angular momentum $\ell \sim 1$. The subsequent infracolor (and possibly QCD) "hadronization" stage does not strongly affect the energy and angular momentum of the quirks, so the quirk pair still has $\ell \sim 1$ even when the quirks have large separation (*e.g.* $r \gg \Lambda^{-1}$).

If there are no further interactions that change the quirk angular momentum, then the quirk pair will not have a well-defined angular direction even if it is macroscopic! If the quirks interact with matter (*e.g.* in the detector) their angular position will certainly be determined, but if we are interested in cases with sufficiently large Λ then the typical length of a quirk string will be small (*e.g.* $\lesssim$ Å) and matter interactions cannot "measure" the angular position. In this case, a collider will create the quirk pair in a "Schrödinger cat" state with large-scale ($r \sim m_Q/\Lambda^2 \gg \Lambda^{-1}$) quantum correlations.

Such a situation is not familiar in particle physics, and we will proceed cautiously. In the end, many of the results can be understood from a simple classical picture, but we will derive the results using WKB wavefunctions to take into account the important quantum-mechanical aspects of these states.

5.3 Wavefunction Overlap

We now consider the probability that a highly excited quirk pair can be found sufficiently close together to re-annihilate. This is a standard problem in quantum mechanics, and we review it here to set the stage for the subsequent discussion. Highly excited states can be described using the WKB approximation. The quirk annihilation probability is proportional to the probability to find the quirk pairs within a distance of order m_Q^{-1} of each other. We will estimate this probability using non-relativistic quantum mechanics and simple approximations that are sufficient for our purposes.

We begin with the case $\ell = 0$. We denote the radial Schrödinger wavefunction by $\psi(r)$ and define the reduced wavefunction by

$$y(r) = \frac{\psi(r)}{\sqrt{4\pi}\, r}. \tag{5.1}$$

This satisfies the normalization condition

$$1 = \int_0^r |y(r)|^2 \tag{5.2}$$

and the boundary condition

$$y(0) = 0. \tag{5.3}$$

The time-independent Schrödinger equation can then be written

$$y''(r) = -k^2(r), \tag{5.4}$$

where

$$k(r) = \frac{\sqrt{2\mu_Q}}{\hbar}\sqrt{K - V(r)}\,. \tag{5.5}$$

Here $K = E - 2\mu_Q$ is the kinetic energy, and $\mu_Q = m_Q/2$ is the invariant mass of the reduced system. We temporarily keep $\hbar \neq 1$ to keep track of the classical limit. We are interested in the case of a linear potential, but we will see that the important results of this section are independent of the details of the potential, so we will keep it general.

We approximate the wavefunction of this system by

$$y(r) \simeq \frac{C}{\sqrt{k(r)}} \sin\left[\int_0^r dr'\, k(r')\right] \theta(r_{\max} - r). \tag{5.6}$$

where $r_{\max}$ is the classical turning point, *i.e.*

$$k(r_{\max}) = 0. \tag{5.7}$$

For $r \ll r_{\max}$ this is the WKB wavefunction, and has the correct boundary condition at $r = 0$. The boundary condition at the classical turning point is only crudely approximated, but this will not strongly affect the probability to find the particle near the origin. In this approximation, we can compute the normalization constant as

$$1 = |C|^2 \int_0^{r_{\max}} dr \, \frac{1}{k(r)} \sin^2 \left[\int_0^r dr' \, k(r') \right]. \tag{5.8}$$

For highly-excited states, we are averaging over many periods with a slowly-varying potential, so we can replace $\sin^2$ by its average value $\frac{1}{2}$. This gives

$$1 = \frac{\hbar |C|^2}{\sqrt{8\mu_Q}} \int_0^{r_{\max}} \frac{dr}{\sqrt{K - V(r)}}. \tag{5.9}$$

This is directly related to the time for a classical trajectory to go from $r = 0$ to $r = r_{\max}$:

$$T = \sqrt{\frac{\mu_Q}{2}} \int_0^{r_{\max}} \frac{dr}{\sqrt{K - V(r)}}. \tag{5.10}$$

For a linear potential

$$V(r) = \sigma r \tag{5.11}$$

we have

$$T = \frac{\sqrt{2\mu_Q K}}{\sigma}. \tag{5.12}$$

However, it is more insightful to leave the results in terms of T as we will see. We therefore have

$$|C|^2 = \frac{2\mu_Q}{\hbar T}. \tag{5.13}$$

We now estimate the probability to find the quirks within a distance r_0 of each other:

$$\text{Prob}(r \leq r_0) = \int_0^{r_0} dr \, |y(r)|^2. \tag{5.14}$$

Near the origin, the wavefunction is oscillating with the de Broglie wavelength

$$\lambda_0 = \frac{2\pi\hbar}{\sqrt{2\mu_Q K}}. \tag{5.15}$$

For $r_0 \gg \lambda_0$ the integral averages over many periods, and we can again replace the $\sin^2$ term by its average value of $\frac{1}{2}$:

$$\text{Prob}(r \le r_0) \simeq \tfrac{1}{2}|C|^2 \int_0^{r_0} \frac{1}{k(r)} = \frac{\Delta t}{T}, \tag{5.16}$$

where

$$\Delta t = \sqrt{\frac{\mu_Q}{2}} \int_0^{r_0} \frac{dr}{\sqrt{K - V(r)}} \tag{5.17}$$

is the classical time to go from $r = 0$ to $r = r_0$ and we have used Eq. (5.13) to eliminate C. This is the result familiar from quantum mechanics textbooks that in a highly excited state the probability to find a particle at the origin is proportional to the fraction of time that a classical orbit spends there.

In the opposite limit $r_0 \ll \lambda_0$ we can use the approximation

$$\sin\left[\int_0^r dr'\, k(r')\right] \simeq \sin k_0 r \simeq k_0 r, \tag{5.18}$$

where $k_0 = 2\pi/\lambda_0$. Since the wavefunction at the origin is

$$\psi(0) = C\sqrt{\frac{k_0}{4\pi}} \tag{5.19}$$

this gives

$$\text{Prob}(r \le r_0) = |C|^2 \int_0^{r_0} k_0 r^2 = |\psi(0)|^2 V, \tag{5.20}$$

where $V = \frac{4}{3}\pi r_0^3$ is the volume of the region of interest. This is the result familiar from positronium and quarkonium physics that the $\ell = 0$ annihilation probability is proportional to the wavefunction at the origin.

The results Eqs. (5.20) and (5.16) are very different parametrically. For $r_0 \gg \lambda_0$ the result is classical and therefore independent of $\hbar$, which is not the case for $r_0 \ll \lambda_0$. Also, for $r_0 \gg \lambda_0$ the probability goes as r_0 (since $\Delta t \sim r_0/v$ where v is the velocity of the classical trajectory near the origin), while for $r_0 \ll \lambda_0$ the probability goes as r_0^3.

We will be mainly interested in the limit $K \ll \mu_Q$, where $r_0 \ll \lambda_0$. From Eqs. (5.20) and (5.13) we have

$$|\psi(0)|^2 = \frac{\sqrt{2\mu_Q^3 K}}{2\pi T} = \frac{m_Q^2 \beta}{4\pi T}, \tag{5.21}$$

where we have expressed the result in terms of the physical quirk mass and the velocity of a single quirk at production, given by

$$\beta = \left(\frac{2K}{m_Q}\right)^{1/2}. \tag{5.22}$$

For the majority of events $\beta \sim 1$ and therefore $|\psi(0)|^2 \sim T^{-1}$. As we will see, this means that for highly excited quirk bound states there is a definite annihilation probability per classical crossing. Eq. (5.12) shows that $T \propto \beta$, so the probability is nonzero at threshold.

It is straightforward to include the effects of nonzero orbital angular momentum. The angular momentum barrier means that classically the particles have a distance of closest approach given by

$$r_{\rm min} = \frac{\ell}{\sqrt{2m_Q K}} \sim \ell \lambda_0, \tag{5.23}$$

where ℓ is the angular momentum. (We are setting $\hbar = 1$ again.) For $r \le r_0 \ll \lambda_0 \lesssim r_{\rm min}$ we can use the approximation

$$y_\ell(r) \simeq C_\ell r^{\ell+1}. \tag{5.24}$$

We can determine the coefficients C_ℓ by matching onto the wavefunction for $r \gtrsim r_{\rm min}$. Since $r_{\rm min} \gtrsim \lambda_0$, the sine function in the wavefunction is of order 1, and we have

$$y_\ell(r_{\rm min}) \sim \frac{C}{k(r_{\rm min})} \sim C_\ell r_{\rm min}^{2\ell+1}. \tag{5.25}$$

With this approximation we obtain

$$\text{Prob}(r \le r_0) \sim \frac{1}{2\ell+3}\left(\frac{\mu_Q}{K}\right)^{1/2} \frac{r_0^{2\ell+3}}{r_{\rm min}^{2\ell+2}} \frac{1}{T}. \tag{5.26}$$

For $r_0 \sim m_Q^{-1}$ this is suppressed compared to the $\ell = 0$ case by

$$\frac{\text{Prob}_{\ell\neq 0}(r \le m_Q^{-1})}{\text{Prob}_{\ell=0}(r \le m_Q^{-1})} \sim \frac{1}{\ell}\left(\frac{\beta}{\ell}\right)^{\ell+1}. \tag{5.27}$$

This suppression means that annihilation is dominated by small ℓ.

5.4 Annihilation Rates

We now use the results above to compute the quirk annihilation rates. For now we neglect the effects of interactions with matter, non-perturbative interactions, and radiation. We work in the highly excited regime $\alpha^2 m_Q \ll K \ll m_Q$. Our results should be approximately valid for $K \lesssim m_Q$, the regime where the majority of quirk pairs are produced. In this regime, the state is sufficiently excited to use the WKB approximation of the previous subsection, but the de Broglie wavelength of the quirk is larger than the distance $r_0 \sim m_Q^{-1}$ over which the annihilation takes place. As we reviewed above, the probability to find the quirks near the origin is dominated by the $\ell = 0$ partial wave, and is proportional to $|\psi(0)|^2$. The density of particles within the range of the annihilation cross section is therefore $|\psi(0)|^2$, and the annihilation rate is

$$\Gamma = |\psi(0)|^2 \sigma v_{\rm rel}, \tag{5.28}$$

where σ is the annihilation cross section and $v_{\rm rel}$ is the relative velocity of the quirks in their center of mass frame. The wavefunction at the origin is given by Eq. (5.21), and is proportional to $1/T$, where T is the classical time for the quirks to go from $r = 0$ to $r = r_{\rm max}$. The annihilation probability per classical crossing is therefore

$$P = 2T\Gamma = \frac{m_Q^2 \beta}{2\pi} \sigma v_{\rm rel}. \tag{5.29}$$

Note that all dependence on the potential has dropped out, so the time scale for annihilation is set by the classical crossing time.

The annihilation cross sections can be computed perturbatively. To get numerical factors right, note that the spin of the quirks is not correlated, and so we must average over intial spins. Similarly, the QCD color of colored quirk pairs is uncorrelated, so we average over quirk colors. On the other hand, quirks are in an infracolor singlet state because they are connected by an infracolor string.

For quirks carrying QCD color, we then have

$$\Gamma(Q\bar{Q} \to gg) = \frac{16 N_{\rm IC}}{27} \frac{2\pi\alpha_3^2}{m_Q^2} |\psi(0)|^2, \tag{5.30}$$

$$\Gamma(Q\bar{Q} \to u\bar{u}) = \frac{2 N_{\rm IC}}{9} \frac{\pi\alpha_3^2}{m_Q^2} |\psi(0)|^2, \tag{5.31}$$

where $\sigma v_{\rm rel}$ has been replaced by its threshold value. The QED annihilation processes are

$$\Gamma(Q\bar{Q} \to \gamma\gamma) = \frac{N_{\rm IC} e_Q^4}{N_{\rm C}} \frac{2\pi\alpha^2}{m_Q^2} |\psi(0)|^2, \tag{5.32}$$

$$\Gamma(Q\bar{Q} \to \gamma^* \to e^+e^-) = \frac{N_{\rm IC} e_Q^2}{N_{\rm C}} \frac{\pi\alpha^2}{m_Q^2} |\psi(0)|^2, \tag{5.33}$$

where e_Q is the electric charge of the quirk and $N_{\rm C}$ is the number of QCD colors of the quirk (so $N_{\rm C} = 1$ if the quirks are color singlets). We have neglected the contribution from Z boson exchange, which gives a small correction. There are similar expressions for annihilation through a W in the case where the electric charge of the quirks differs by one unit.

For quirks carrying both QCD color and electric charge there is a potentially interesting mixed annihilation to gluons and photons with rate

$$\Gamma(Q\bar{Q} \to g\gamma) = \frac{4 N_{\rm IC} e_Q^2}{9} \frac{2\pi\alpha\alpha_3}{m_Q^2} |\psi(0)|^2. \tag{5.34}$$

This motivates searches for photon-jet resonances at colliders.

There is also annihilation to infracolor gluons, which gives

$$\Gamma(Q\bar{Q} \to \text{infracolor}) = \frac{N_{\rm IC}^2 - 1}{4 N_{\rm IC} N_{\rm C}} \frac{2\pi\alpha_{\rm IC}^2}{m_Q^2} |\psi(0)|^2. \tag{5.35}$$

For $\Lambda \lesssim 10$ GeV, the infracolor glueballs are stable on collider scales and this is an invisible decay. The gauge couplings in Eqs. (5.30)–(5.35) are to be evaluated at a renormalization scale m_Q. For the infracolor coupling, we approximate

$$\alpha_{\rm IC}(m_Q) \simeq \frac{6\pi}{11 N_{\rm IC} \ln 4m_Q/\Lambda_{\rm IC}}. \tag{5.36}$$

Here we estimate the scale where the perturbative coupling blows up as $\Lambda_{\rm IC}/4$. (In QCD, this scale is $\simeq 250$ MeV, while the scale of strong interactions is $\simeq$ GeV.)

The annihilation probability per classical crossing time is important in comparing the annihilation rate with other energy loss mechanisms. For colored quirks, the annihilation into quarks and gluons dominates. The probability of annihilation per classical crossing is

$$P_{\rm QCD} = 2T\Gamma_{\rm QCD} = \frac{32 N_{\rm IC}}{27} \alpha_3^2 \beta \sim \frac{1}{40}, \tag{5.37}$$

where we have assumed that the quirks can annihilate into all 6 quark flavors, and we assumed $N_{\rm IC} = 3$ and $\beta \sim 1$. For uncolored quirks with opposite charge, the probability per classical crossing to annihilate is

$$P_{\rm QED} = N_{\rm IC}(6e_Q^2 + e_Q^4)\alpha^2\beta \sim \frac{1}{780}, \tag{5.38}$$

where we have used $e_Q = 1$, $N_{\rm IC} = 3$ for the numerical estimate. The annihilation probability per classical crossing to annihilate to infracolor gluons is

$$P_{\rm inv} = \frac{N_{\rm IC}^2 - 1}{2N_{\rm IC}} \alpha_{\rm IC}^2 \beta \sim \frac{1}{160} \frac{1}{[1 - 0.12 \ln(\Lambda_{\rm IC}/{\rm GeV})]^2}, \tag{5.39}$$

where we assume uncolored quirks with $N_{\rm IC} = 3$ and $m_Q \sim$ TeV. We see that the annihilation into visible final states is significant even for uncolored states with large values of Λ. These results will be useful in assessing the probability that quirks undergo prompt annihilation.

Another important quantity is the branching ratio for colored quirks to annihilate to leptons and photons. We have

$$\frac{\Gamma(Q\bar{Q} \to \mu^+\mu^-)}{\Gamma(Q\bar{Q} \to jj)} = \frac{9}{68} \frac{e_Q^2 \alpha^2}{\alpha_3^2} \simeq 1.4 \times 10^{-4}, \tag{5.40}$$

$$\frac{\Gamma(Q\bar{Q} \to \gamma\gamma)}{\Gamma(Q\bar{Q} \to jj)} = \frac{9}{34} \frac{e_Q^4 \alpha^2}{\alpha_3^2} \simeq 3 \times 10^{-5}, \tag{5.41}$$

where we have taken $e_Q = \frac{1}{3}$ for the numerical values. These branching ratios are discouragingly small.[2] On the other hand, the branching ratio to photon plus jets is

$$\frac{\Gamma(Q\bar{Q} \to g\gamma)}{\Gamma(Q\bar{Q} \to jj)} = \frac{6}{17} \frac{e_Q^2 \alpha}{\alpha_3} \sim 3 \times 10^{-3}, \tag{5.42}$$

where we again take $e_Q = \frac{1}{3}$. This is somewhat more encouraging.

The accuracy of the estimates above can easily be improved by incorporating the behavior of the cross section at threshold and relativistic effects. We leave this to future work.

The annihilation probabilities computed above are relevant when there are no interactions that can change the angular momentum of the quirks. We now consider these interactions to see whether they are in fact negligible.

5.5 Non-perturbative QCD Interactions

We now consider the effects of non-perturbative QCD interactions on colored quirk annihilation. Colored quirks are surrounded by a cloud of non-perturbative QCD "brown muck" with size $R_{\rm had} \sim \Lambda_{\rm QCD}^{-1}$. Interactions between the brown muck of

[2]These branching fractions are lower than the corresponding ones for the Upsilon decays mainly because the initial state is not a color singlet. This opens additional colored channels and enhances the strong decay rate.

the quirks are important because they have a larger cross section than the hard annihilation processes considered previously. Although they do not result in the annihilation of the quirk pair, they can change the angular momentum of the quirk pair and affect the probability for hard annihilation.

We assume that $L \gg R_{\rm had}$, so that we can treat the quirk hadrons as well-separated particles moving under the influence of an infracolor string. This requires

$$E \gtrsim \frac{\Lambda^2}{\Lambda_{\rm QCD}}. \tag{5.43}$$

For example, for $\Lambda \sim$ GeV this requires only $E \gtrsim$ GeV, a mild requirement for hard production. For $\Lambda \gtrsim 10$ GeV, this starts to be a significant constraint, and our results will be qualitatively reliable at best.

The brown muck will interact only when the quirks come within a distance of order $R_{\rm had}$. We are interested in inelastic processes (*e.g.* pion emission) that can change the energy and angular momentum of the bound state. The typical energy transfer from the bound state can be estimated from

$$\Delta E \sim F \Delta r \sim \Lambda_{\rm QCD}^2 R_{\rm had} \sim \Lambda_{\rm QCD}. \tag{5.44}$$

The momentum transfer can in principle be larger if the quirks are moving slowly:

$$\Delta p \sim F \Delta t \sim \Lambda_{\rm QCD}^2 \frac{R_{\rm had}}{v} \sim \frac{\Lambda_{\rm QCD}}{v}. \tag{5.45}$$

However, for pion emission $\Delta p \sim \Delta E$, so energy and momentum transfer are of order $\Lambda_{\rm QCD}$. We expect such processes to have a geometric cross section of order $\pi R_{\rm had}^2$, since there is no small parameter suppressing the interaction probability.[3] Note that the large kinetic energy carried by the quirk is not transfered in the interaction, and does not suppress the interaction probability.

A geometrical cross section is equivalent to saturating unitarity for all partial waves up to

$$\ell_{\rm max} \sim m_Q v R_{\rm had} \sim (m_Q E)^{1/2} R_{\rm had}. \tag{5.46}$$

Unless we are very close to threshold we have $\ell_{\rm max} \gg 1$, and so the partial wave cross section will approximately saturate unitarity unless the angular momentum is very large. This means that the interaction will take place with of order unit probability whenever the quirks come within a distance of order $R_{\rm had}$ or less. We therefore expect

[3] If the number of QCD colors is regarded as a large parameter, the probability for interaction is of order $1/N_{\rm C}$. We will neglect large $N_{\rm C}$ effects in the following.

that a brown muck interaction transfering energy and momentum of order $\Lambda_{\rm QCD}$ will take place roughly once every crossing time, as long as $\ell \lesssim \ell_{\rm max}$.

We can understand this result using a simple quantum-mechanical model. We model the brown muck as a particle (a constituent quark) of mass $\sim \Lambda_{\rm QCD}$ bound to each quirk by a potential that represents the effects of the QCD interactions. The wavefunction for the system is then a function of the relative coordinate of the quirks $\vec{r}$ and the coordinates of the constituent quarks relative to the associated quirk $\vec{\rho}_{1,2}$. The wavefunction is assumed to take the approximate form

$$\Psi(\vec{r}, \vec{\rho}_1, \vec{\rho}_2) \sim \psi(r)\chi(\rho_1)\chi(\rho_2), \tag{5.47}$$

where $\psi(r)$ is the quirk wavefunction, and $\chi(\rho)$ is the consituent quark wavefunction. This factorized form is justified for $r \gg R_{\rm had}$ where the quirks are well separated. The constituent quark wavefunction $\chi(\rho)$ is nonzero only for $\rho \lesssim R_{\rm had}$. It is convenient to normalize it so that

$$\int d^3\rho \, |\chi(\rho)|^2 \sim R_{\rm had}^3. \tag{5.48}$$

We then have (see Subsection 5.3)

$$\psi(r) \simeq \frac{C'}{r} \frac{1}{\sqrt{k(r)}} \sin\left[\int_0^r dr' \, k(r')\right]. \tag{5.49}$$

We are using an $\ell = 0$ wavefunction, which will have the right qualitative behavior as long as $\ell \ll \ell_{\rm max}$. Normalizing the wavefunction gives

$$|C'|^2 \sim \frac{m_Q}{\hbar R_{\rm had}^6 T}, \tag{5.50}$$

where T is the classical crossing time. Here we make the same approximations as previously for the quirk wavefunction. We can then compute the probability that the brown muck particles are within a distance $R_{\rm had}$ from each other:

$$\begin{aligned} {\rm Prob}(|\vec{r} + \vec{\rho}_1 - \vec{\rho}_2| \le R_{\rm had}) &= \frac{|C'|^2}{2k_0} \int d^3r \, \frac{1}{r^2} \int d^3\rho_1 \, |\chi(\rho_1)|^2 \int d^3\rho_2 \, |\chi(\rho_2)|^2 \\ &\qquad \times \theta(R_{\rm had} - |\vec{r} + \vec{\rho}_1 - \vec{\rho}_2|) \qquad (5.51) \\ &\sim |C'|^2 \frac{\hbar R_{\rm had}^7}{(m_Q E)^{1/2}} \sim \frac{R_{\rm had}/v}{T}, \qquad (5.52) \end{aligned}$$

where $v \sim (E/m_Q)^{1/2}$ is the classical quirk velocity at the origin and we have again used the fact that the Compton wavelength of the the heavy quirk is much smaller

than $R_{\rm had}$. This is the fraction of the time that the quirks are within a distance $R_{\rm had}$. To find the reaction rate, we must find the density of incident particles over the range of the interaction. This is

$$\rho \sim \frac{R_{\rm had}/v}{T} \frac{1}{R_{\rm had}^3} \sim \frac{1}{R_{\rm had}^2 v T}, \tag{5.53}$$

so the reaction rate is

$$\Gamma \sim \rho v \sigma \sim \frac{1}{R_{\rm had}^2 v T} v R_{\rm had}^2 \sim \frac{1}{T}. \tag{5.54}$$

We are again led to the conclusion that these interactions occur roughly once per classical crossing.

One important effect of these interactions is that it changes the angular momentum state of the quirk pair. The quirks are produced in a state with angular momentm $\ell \sim 1$, *i.e.* a highly spherical quantum state in which the angular position of the quirks has nearly maximal uncertainty. The hadrons that are emitted eventually interact with matter far from the detector, and therefore can be thought of as having a definite direction. The fact that the angular momentum state of the hadrons is entangled with that of the quirk pair means that this reduces the quantum uncertainty in the the angular direction of the quirk pair. In the traditional textbook language of quantum mechanics, the angular position of the quirks gradually becomes "measured" by the repeated "measurement" of the pion angular positions.[4] A proper treatment of this process using the ideas of quantum decoherence is beyond the scope of the present work, and we will only make some simple estimates here.

The angular momentum transfered to the emitted hadrons in a single brown muck interaction is of order

$$\Delta \ell \sim R_{\rm had} \Delta p \sim 1. \tag{5.55}$$

Assuming that the interaction is equally likely to raise or lower the angular momentum, we have $\ell \sim \sqrt{N}$ after N such interactions.[5] The hard annihilation cross section falls rapidly for $\ell \gtrsim$ few, so there is a competition between hard annihilation, which wants to eliminate the bound state in a small number of classical crossing times, and the non-perturbative QCD interactions, which tend to increase the average angular momentum, and therefore suppress hard annihilation.

[4] We are neglecting possible interactions of the quirks with matter, which would directly "measure" the angular position of the quirks. This discussion is therefore applicable to the case where the string is sufficiently short that matter interactions are unimportant.

[5] The angular momentum is positive semi-definite, but this is taken care of in the random walk by simply identifying $\pm \ell$.

We can illustrate these points with a simple quantum mechanical toy model. We work in 2 dimensions, where the angular momentum eigenstates are simply $e^{im\theta}$, where θ is the polar angle and m is an integer. We can simplify the model further by restricting the particles to a circle, so there is no radial wavefunction to worry about. We assume that there is a process by which a "quirk bound state" in an angular momentum m state emits a "pion" that also lives on the circle. The 1-particle wavefunction therefore makes a transition to a 2-particle wavefunction

$$e^{im\theta} \to a_0 e^{im\theta} + a_1 e^{i(m+1)\theta} e^{-i\theta'} + a_{-1} e^{i(m-1)\theta} e^{i\theta'} + \cdots. \tag{5.56}$$

Here θ' is the angular coordinate of the emitted pion. The transition conserves angular momentum since $L = -i(\partial_\theta + \partial_{\theta'})$. The amplitudes $a_0, a_{\pm 1}, \ldots$ can depend on m, but we make the simplifying assumption that they are independent of m. We assume that a_n is significant for $n \sim 1$, so it is sufficient to consider a_0 and $a_{\pm 1}$. Symmetry under $\theta \to -\theta$ then implies that $a_1 = a_{-1}$, and we have simply

$$\psi(\theta) \to \psi'(\theta, \theta') = \Big[a_0 + 2a_1 \cos(\theta - \theta') + \cdots\Big]\psi(\theta). \tag{5.57}$$

We can choose a_0 real without loss of generality. We assume that the pion emission is peaked at $\theta = \theta'$, so that a_1 is mostly real. We now imagine that the bound state repeatedly emits pions, and the angular position of the pions is measured. This corresponds to making the transition Eq. (5.57) and then fixing θ' by picking a value of θ' according to the probability distribution

$$P(\theta') = \int d\theta \, |\psi'(\theta, \theta')|^2. \tag{5.58}$$

Picking θ' in this way then gives a new wavefunction that depends only on θ, which can then undergo further transitions.

This simple toy model captures the basic quantum kinematics of the problem we care about. For example, we can easily see how repeated transitions of the form Eq. (5.57) make the angular position more well-determined. The value of θ' is correlated with the direction of θ, so this tends to make the peak more pronounced. The quantity of most interest to us is the probability to find the bound state in an $m = 0$ state after N transtions. This probability is expected to decrease as $\sim 1/\sqrt{N}$, since each transition changes the maximum angular momentum by ± 1. This is born out by Monte Carlo simulation of this model (See Fig. 8). Although this toy model is a drastic simplification of the system of interest, it illustrates that the expected behavior does arise from quantum mechanics. We therefore expect the same behavior in the realistic system.

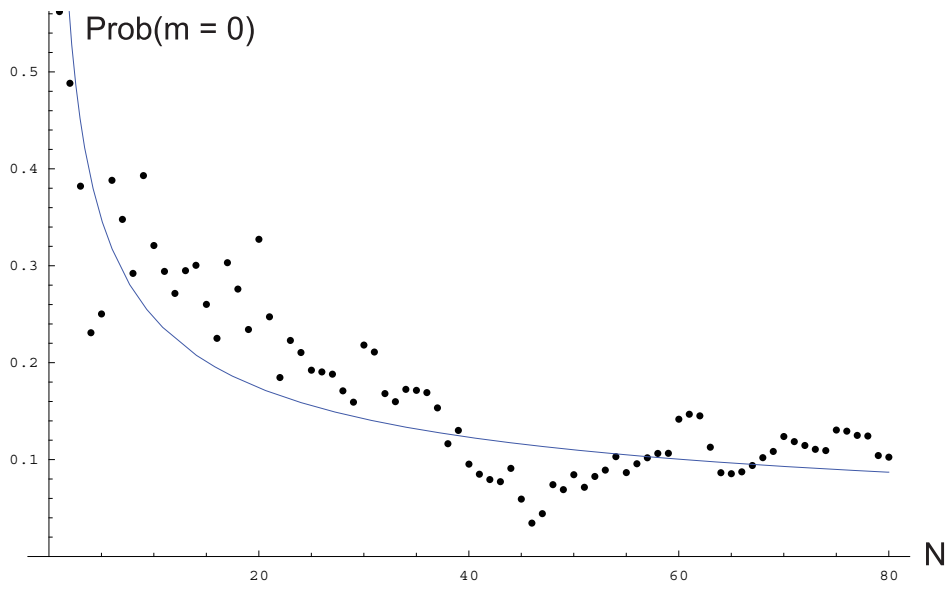

Fig. 8. Monte Carlo simulation of toy model of angular decoherence. The plot shows the probability to find the system in the $m = 0$ angular momentum state after N interactions. The curve is the fit to constant$/\sqrt{N}$.

5.6 Hadronic Fireballs?

The arguments above suggest that a significant fraction of colored quirk pairs lose most of their energy to emission of QCD hadrons. This requires that the quirks do not annihilate for a number of crossings of order $m_Q/\Lambda_{\rm QCD} \sim 10^3$. The non-perturbative QCD interactions remain effective up to very large angular momenta, of order $\ell_{\rm max} \sim m_Q/\Lambda_{\rm QCD} \sim 10^3$, which takes would take of order 10^6 crossing times to reach according to the random-walk picture. In the meantime, each non-perturbative QCD interaction results in the emission of one (or several) hadrons with total energy $\sim \Lambda_{\rm QCD} \sim$ GeV. This means that the kinetic energy of the bound state ($K \sim m_Q \sim$ TeV) is rapidly converted to $\sim 10^3$ hadrons with energy $\sim$ GeV each: a hadronic "fireball."

We can obtain a simple estimate of the fraction of events of this type by assuming that the quirk survival probability at the $n^{\rm th}$ crossing is $(1-P/\sqrt{n})$, where $P \sim 1/360$ is the s-wave annihilation probability. The probability to survive for 10^3 crossings is then approximately 85%.

When the quirks finally annihilate, they are essentially at rest in their center of mass frame, so the annihilation products appear as a narrow resonance with mass $2m_Q$. The intrinsic width will be due to the fact that the final annihilation will take place from a distribution of low-lying Coulombic "quirkonium" states. The width will therefore be of order the spacing of low-lying Coulombic energy levels, given by

$$\Delta E \sim \alpha_{\rm IC}^2(m_Q)\frac{m_Q}{2} \sim 3\ {\rm GeV}\left(\ln\frac{m_Q/{\rm TeV}}{\Lambda/{\rm GeV}}\right)^{-2}. \tag{5.59}$$

This also sets the scale for the energy emission during the final stages of the decay, which we see is only slightly larger than the QCD scale.

The time for this process is set by the classical crossing time and the number of interactions required to lose the kinetic energy:

$$c\tau \sim \frac{m_Q}{\Lambda_{\rm QCD}}\frac{m_Q}{\Lambda^2} \sim 10^{-2}\ {\rm cm}\left(\frac{\Lambda}{\rm MeV}\right)^{-2}\left(\frac{m_Q}{\rm TeV}\right)^2. \tag{5.60}$$

We see that the decay may have a displaced vertex for smaller values of Λ.

The dominant decay will be to two jets, which may be a difficult signal due to large backgrounds. The decay to leptons or photons has a suppressed branching ratio, but offers a cleaner signal that may be easier to look for. If energy loss due to QCD interactions is efficient, the final hard annihilation of the quirks will be from a Coulomb-like state that is color and infracolor singlet. This means that there are fewer colored channels compared to the excited annihilation computed in Subsection 5.4. Assuming s-wave annihilation we find

$$\frac{\Gamma(Q\bar{Q}\to\mu^+\mu^-)}{\Gamma(Q\bar{Q}\to{\rm jets})} = 18\frac{e_Q^2\alpha^2}{\alpha_3^2} \simeq 2\times10^{-2}, \tag{5.61}$$

$$\frac{\Gamma(Q\bar{Q}\to\gamma\gamma)}{\Gamma(Q\bar{Q}\to{\rm jets})} = 36\frac{e_Q^4\alpha^2}{\alpha_3^2} \simeq 4\times10^{-3}, \tag{5.62}$$

for $e_Q = \frac{1}{3}$. This looks very promising. The decay to $g\gamma$ is absent, although there is a suppressed decay mode $gg\gamma$.

Since the quirks lose all their kinetic energy before decaying in these events, the decay products will have an invariant mass very close to $2m_Q$. The intrinsic width will be due to the fact that the final annihilation will take place from a distribution of low-lying Coulombic states. These have very small energy differences of order ΔE (see Eq. (5.59)), so the intrinsic width of the resonance is very small.

Can we hope to see the hadronic fireballs associated with these decays? Most of the hadrons are expected to be pions. Muons from charged pion decays will be

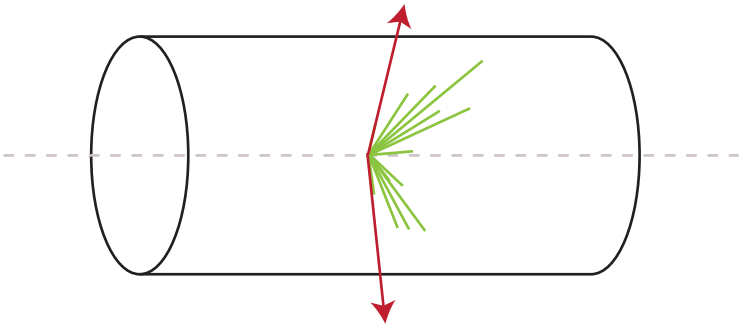

Fig. 9. Schematic depiction of hadronic fireball and hard annihilation into muons. Note that the the asymmetry of the muons and the fireball are in the same direction.

difficult to detect because they are highly curved in the magnetic field of the detector. Neutral pions decay to photons, which may be more promising to detect. The angular distribution of the fireball may aid in distinguishing it from background. Due to the angular decoherence, the quirk pair acquires an angular position in the center of mass frame. We expect that hadron emission is peaked in the direction of the quirk motion, resulting in a doubly-peaked pattern in the center of mass frame. Note that the quirk annihilation is dominantly s-wave, and so the direction of the annihilation products is not correlated with the direction of the original quirk motion. This means that the fireball generally does not line up with the annihilation products. Furthermore, the longitudinal boost of the center of mass system will push both the fireball and the hard annihilation products in the same direction. This is illustrated in Fig. 9.

Although we expect that energy loss due to QCD brown muck is efficient, a significant fraction of quirks annihilate after only a few crossings (see Eq. (5.37)). The branching ratio for these annihilations into leptons or photons are much smaller than the decays above (see Eqs. (5.40) and (5.41)), but may be worth searching for. The width of this enhancement is of order m_Q, and the shape is determined from the 2-particle invariant mass distribution of the produced quirks. This gives an additional handle on these events.

5.7 Non-perturbative Infracolor Interactions

We now consider non-perturbative infracolor interactions of the quirks. There are many analogies with the non-perturbative QCD interactions of colored quirks discussed in the previous subsection, so our discussion will be brief and highlight the

important differences.

The infracolor "brown muck" has a geometrical cross section for interaction, so we also expect ~ 1 interaction per classical crossing time. As argued in Subsection 3.3, radiation of infracolor glueballs takes place only while the quirk separation is less than or of order Λ^{-1}. The non-perturbative infracolor interactions will therefore give rise to the emission of only ~ 1 infracolor gluons with total energy $\sim \Lambda$.

One important difference with the QCD case is that the infracolor hadrons generally do not interact after they are emitted, and therefore their angular position is probably not "measured" on time scales relevant for colliders. The cross section for an infracolor glueball with energy $\sim \Lambda$ to scatter *e.g.* via $\gamma g \to \gamma g$ is of order

$$\sigma \sim \frac{1}{16\pi}\frac{\Lambda^6}{m_Q^8} \sim 10^{-16}\sigma_W \left(\frac{\Lambda}{\mathrm{GeV}}\right)^4 \left(\frac{m_Q}{\mathrm{TeV}}\right)^{-8}, \tag{5.63}$$

where $\sigma_W \sim \Lambda^2/16\pi M_W^2$ is a typical weak cross section. However, even if we assume that quantum coherence is maintained between the angular wavefunction and the wavefunction of the emitted infracolor hadrons, we still expect the probability to find the quirks in a low partial wave after N interactions to go like $1/\sqrt{N}$, since the quirk wavefunction is "random-walking" away from low partial waves with each interaction. We therefore expect these interactions to suppress annihilation similarly to the QCD case.

Another potentially important difference from the QCD case is the fact that the glueball mass is of order the strong interaction scale, so it is possible that glueball emission is kinematically suppressed. For example, lattice simulations of $SU(3)$ gauge theory indicate that the mass of the 0^{++} glueball is 3.6 times heavier than the square root of the string tension [18]. Although there is no parametric suppression, one should keep in mind the possibility that there is some kinematic suppression of glueball production. The amplitude to emit a hard infracolor gluon is shown in Fig. 10. The amplitude has one off-shell gluon and one off-shell heavy quirk line, and therefore is suppressed by $1/q^3$ where q is the hard momentum transfer, so the cross section is down by $1/q^6$ at large q. If this behavior sets in already at the glueball mass, we can imagine a suppression of order $(\frac{1}{3})^6 \sim 10^{-3}$ in the cross section.

We therefore consider the two extreme scenarios: one where there is no suppression, and one where non-perturbative infracolor interactions are effectively absent. In the first case, there can be significant energy loss to infracolor gluons for sufficiently large Λ, which gives rise to unobservable missing energy. In the second case, other mechanisms of energy loss (*e.g.* radiation) may be important.

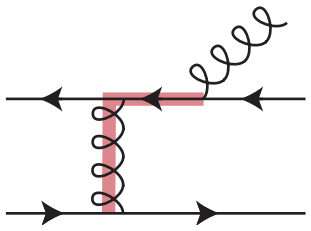

Fig. 10. Diagram contributing to infracolor energy loss at high momentum transfer. Hard internal lines are shaded.

5.8 Magnetic Field

Another effect that can be important in preventing annihilation is the magnetic field in the detector, of order Tesla at the Tevatron and LHC. The quirk center of mass frame is boosted relative to the lab frame, so there will be an electric field in this frame. This electric field will typically have a component perpendicular to the direction of the quirk motion, which will give rise to a repulsive force between oppositely charged quirks. This in turn will generate a classical separation after one oscillation of order

$$\Delta r \sim aT^2 \sim \frac{v_{\rm cm} B}{m_Q} \left(\frac{m_Q}{\Lambda^2}\right)^2 . \tag{5.64}$$

where $v_{\rm cm}$ is the velocity of the center of mass frame. Demanding that this is larger than m_Q^{-1} (and assuming $v_{\rm cm} \sim 1$) gives

$$\Lambda \lesssim \text{MeV} \left(\frac{B}{\text{Tesla}}\right)^{1/4} \left(\frac{m_Q}{\text{TeV}}\right)^{1/2} . \tag{5.65}$$

Since magnetic fields at Tevatron and LHC colliders are of order Tesla, we expect that this will prevent re-annihilation for $\Lambda \lesssim$ MeV.

This mechanism will be ineffective for special kinematical configurations. The induced electric field vanishes if the center of mass of the system is along the magnetic field, that is the beam direction. The induced electric field does not give rise to a transverse separation between the quirks if their motion in the center of mass frame is along the magnetic field. It is straightforward to check that the magnetic field in the center of mass frame does not cause a transverse quirk separation to leading order in the magnetic field. Therefore, if the magnetic field is the only effect preventing annihilation, there may be some events in corners of kinematic phase space that annihilate.

5.9 Electromagnetic Radiation

The rate of electromagnetic radiation can be estimated from the Larmor formula

$$\dot{E} \sim \alpha(\ddot{d})^2, \tag{5.66}$$

where d is the dipole moment of the charge distribution (with the charge factored out). A perfect s-wave has $d \equiv 0$, but even if the total angular momentum is $\ell \sim 1$ the dipole moment will be of order $r_{\max}$. The energy radiated in a crossing time T is therefore

$$\Delta E \sim \dot{E}T \sim \alpha \left(\frac{r_{\max}}{T}\right)^2 \sim \frac{\alpha}{T}. \tag{5.67}$$

Since the typical photon energy radiated is of order $E_\gamma \sim 1/T$, this means that there are of order α photons emitted in each classical crossing. The number of crossings required to lose energy of order m_Q to electromagnetic radiation is therefore of order

$$N_\gamma \sim \frac{m_Q}{\dot{E}}\frac{1}{T} \sim \frac{m_Q^2}{\alpha\Lambda^2} \sim 10^8 \left(\frac{\Lambda}{\text{GeV}}\right)^{-2} \left(\frac{m_Q}{\text{TeV}}\right)^2. \tag{5.68}$$

This is much larger than the number of crossings to annihilate. Brown muck interactions can prevent annihilation, but then they will be the dominant energy loss mechanism since $E_\gamma \ll \Lambda$. We conclude that electromagnetic energy loss is unlikely to be important.

6 Mesoscopic Strings

We now consider the case where the strings are too small to be resolved in a detector (roughly $L \lesssim$ mm), but are large compared to atomic scales ($L \gtrsim$ Å). This corresponds to roughly

$$10 \text{ keV} \lesssim \Lambda \lesssim \text{MeV} \tag{6.1}$$

for $m_Q \sim$ TeV. In this case, the quirk-antiquirk pair will appear as a single particle in the detector.

For mesoscopic strings, we can no longer take for granted that matter interactions will randomize the angular momentum and prevent the quirks from annihilating. In other words, we need to know whether the bound state lives long enough to appear in the detector. The interaction region has an inner radius of order cm with very high vacuum, and matter interactions are not important there. We must therefore consider other mechanisms to prevent annihilation.

An important effect in preventing annihilation is the magnetic field. In the quirk center of mass frame, there will be an electric field with a component perpendicular to the direction of quirk motion that gives rise to a separation of classical quirk trajectories after one oscillation of order

$$\Delta r \sim aT^2 \sim \frac{v_{\rm cm} B}{m_Q} \left(\frac{m_Q}{\Lambda^2}\right)^2 . \tag{6.2}$$

where $v_{\rm cm}$ is the velocity of the center of mass frame. Demanding that this is larger than m_Q^{-1} (and assuming $v_{\rm cm} \sim 1$) gives

$$\Lambda \lesssim {\rm MeV} \left(\frac{B}{\rm Tesla}\right)^{1/4} \left(\frac{m_Q}{\rm TeV}\right)^{1/2} . \tag{6.3}$$

Since magnetic fields at Tevatron and LHC colliders are of order Tesla, we expect that this will prevent re-annihilation for $\Lambda \lesssim$ MeV.

While the quirk pair is inside the beam pipe, the only efficient mechanism for energy loss and change of angular momentum is the brown-muck interactions discussed in the previous section. For colored quirks, these lead to a decay length (see Eq. (5.60))

$$c\tau \sim {\rm cm} \left(\frac{\Lambda}{100\ {\rm keV}}\right)^{-2} \left(\frac{m_Q}{\rm TeV}\right)^2 \tag{6.4}$$

while for uncolored quirks

$$c\tau \sim 10\ {\rm cm} \left(\frac{\Lambda}{\rm MeV}\right)^{-3} \left(\frac{m_Q}{\rm TeV}\right)^2 . \tag{6.5}$$

We see that these decays can allow the quirk bound state to survive for distances of order cm. As discussed in the previous section, the efficiency of this mechanism of energy loss is uncertain, particularly for the infracolor energy loss. The decay lengths may therefore be significantly longer than these estimates.

Once the bound state reaches the beam pipe, matter interactions are efficient at randomizing the angular momentum and preventing annihilation. For example, a single collision with an electron transfers momentum of order m_e, which changes the angular momentum by

$$\Delta \ell \sim m_e L \sim m_e \frac{m_Q}{\Lambda^2} \sim 10^3 \left(\frac{\Lambda}{\rm MeV}\right)^{-2} \left(\frac{m_Q}{\rm TeV}\right) . \tag{6.6}$$

For the remainder of this section we will assume that the bound state appears as a stable particle in the detector. In order to see the bound state, it must be produced in

association with a hard jet or photon so that the bound state is off the beam axis. If the bound state has a net electromagnetic charge, it will leave a track in the detector. The signal is then a single heavy stable particle recoiling against a hard jet or photon.

The most interesting aspect of these events is the fact that the mass of the bound state is the invariant mass of the quirk-antiquirk pair. This has a broad distribution, so the mass of the bound state differs by order 1 event by event. The mass of a heavy stable charged particle can be measured event by event by a combination of its bending in a magnetic field and time of flight. This has been studied at LHC [19], with the conclusion that the mass can be determined at the few percent level for events with $0.6 \lesssim \beta \lesssim 0.8$. Observation of stable particles with the mass spectrum given by the 2-particle invariant mass spectrum would be essentially a direct observation of strings.

7 Microscopic Strings

We now consider the signals for microscopic strings, roughly $L \lesssim$ Å, corresponding roughly to

$$\text{MeV} \lesssim \Lambda \lesssim m_Q/\text{few}. \tag{7.1}$$

As we have seen above, in this regime interactions with matter and the magnetic field of the detector do not prevent the quirks from annihilating. These signals have been largely discussed in Section 5, so our discussion here is mainly a summary of this discussion.

7.1 Colored Quirks

We begin with colored quirks, which are the ones most copiously produced at a hadron collider. Most of the quirks produced above threshold will undergo hard annihilation without significant energy loss. Colored quirks will annihilate dominantly into jets, but may have branching fractions into leptons or photons at the percent level (see Subsection 5.4). These events will have a broad distribution essentially given by the perturbative 2-particle invariant mass spectrum of the quirks.

A significant fraction (a few percent) of colored quirk pairs will lose most of their kinetic energy energy because of interactions of the non-perturbative QCD and/or infracolor interactions. The condition for non-perturbative QCD interactions to dominate is naïvely $\Lambda_{\text{QCD}} > \Lambda$, but there is significant uncertaintly in the efficiency of the non-perturbative infracolor energy loss. If the QCD interactions dominate, an energy

of order $2m_Q$ will be radiated as light QCD hadrons (mainly pions) each with energy of order GeV: a hadronic fireball.

The total invariant mass distribution of the quirk decay products is therefore a broad distribution approximating the 2-particle invariant mass distribution with a narrow peak superimposed. This distribution can be found in jets, but also (with reduced rate) in lepton or photon pairs. Detailed study of this signal would be very interesting.

7.2 Uncolored Quirks

Uncolored electromagnetically charged quirks will annihilate dominantly into infracolor glueballs for the range of Λ of interest. Infracolor glueballs are unobservable unless $\Lambda \gtrsim 50$ GeV (see Eq. (2.3)), in which case they decay inside the detector. However, there will be branching ratio typically of order 10% for annihilation into visible states (see Eqs. (5.38) and (5.39)). We can have annihilation to photon pairs, or through a virtual photon, Z, or W. The final state will therefore include a significant fraction of photon and lepton pairs, which are readily observable.

Non-perturbative infracolor interactions will tend to bring the quirks to rest before they annihilate. If these are fully efficient, they will radiate of order one infracolor glueball with energy of order Λ and total angular momentum of order 1 once per classical crossing time. However, glueball masses are themselves of order Λ, so it is possible that there is a kinematic suppression of this process. Given our lack of understanding of this non-perturbative dynamics, it makes sense to consider both the case where these interactions are efficient and inefficient.

Hard annihilation of excited uncolored quirks requires of order 10^2 crossings (see Eq. (5.38)), giving the non-perturbative infracolor interactions plenty of time to randomize the angular momentum. If these interactions are efficient, we therefore expect the majority of these annihilations to take place with the quirks at rest, leading to a very narrow resonance. If these interactions are inefficient, the resonance will be broad with a narrow peak superimposed from the quirks that are produced near threshold.

8 Conclusions

We have seen that massive particles charged under an unbroken non-abelian gauge group give rise to spectacular phenomenology at colliders. These signals are sufficiently exotic that they will almost certainly be missed unless they are searched for. Given the simple nature of these models, it is worthwhile to put some effort in this

direction. The next step will be to produce event generators for this exotic physics that can be used to develop concrete search strategies. Cosmological aspects of these models will also be addressed in a future publication.

Acknowledgements

This paper had a long gestation during a eventful and sometimes difficult time in the life of MAL. He would like to dedicate his work on this paper to the memory of Alexander M. Luty. It is a pleasure to thank the following colleagues for useful discussions and (in most cases) encouragement: Z. Chacko, H.-C. Cheng, A. De Roeck, R. Harnik, H.-S. Goh, S. Nasri, Y. Nomura, M. Peskin, M. Strassler, and J. Terning. We thank J. Evans for generating the quirk production plots. This work was partly performed at the Aspen Center for Physics and the Kavli Institue for Theoretical Physics. This work was partly supported by NSF grant PHY-0652363 and by the Maryland Center for String and Particle Theory.

References

[1] L. B. Okun, JETP Lett. **31**, 144 (1980) [Pisma Zh. Eksp. Teor. Fiz. **31**, 156 (1979)]; Nucl. Phys. B **173**, 1 (1980).

[2] J. D. Bjorken, SLAC-PUB-2372 (1979); S. Gupta and H. R. Quinn, Phys. Rev. D **25**, 838 (1982).

[3] M. J. Strassler and K. M. Zurek, arXiv:hep-ph/0604261.

[4] C. Jacoby and S. Nussinov, arXiv:0712.2681 [hep-ph]; M. A. Luty, J. Kang, and S. Nasri, to appear.

[5] A. Manohar and H. Georgi, Nucl. Phys. B **234**, 189 (1984).

[6] C. Boehm, D. Hooper, J. Silk, M. Casse and J. Paul, Phys. Rev. Lett. **92**, 101301 (2004) [arXiv:astro-ph/0309686].

[7] S. Dimopoulos and L. J. Hall, Phys. Lett. B **196**, 135 (1987).

[8] K. S. Babu, I. Gogoladze and C. Kolda, arXiv:hep-ph/0410085.

[9] G. Burdman, Z. Chacko, H. S. Goh and R. Harnik, JHEP **0702**, 009 (2007) [arXiv:hep-ph/0609152].

[10] J. Schwinger, Phys. Rev. 82, 664 (1951); A. Casher, H. Neuberger and S. Nussinov, Phys. Rev. D **20**, 179 (1979).

[11] A. Sommerfeld, Ann. Phys. 11 257 (1931).

[12] R. Sundrum, arXiv:hep-ph/9702306.

[13] M. Luscher and P. Weisz, JHEP **0207**, 049 (2002) [arXiv:hep-lat/0207003].

[14] K. Hamaguchi, Y. Kuno, T. Nakaya and M. M. Nojiri, Phys. Rev. D **70**, 115007 (2004) [arXiv:hep-ph/0409248]; J. L. Feng and B. T. Smith, Phys. Rev. D **71**, 015004 (2005) [Erratum-ibid. D **71**, 019904 (2005)] [arXiv:hep-ph/0409278]; A. Arvanitaki, S. Dimopoulos, A. Pierce, S. Rajendran and J. G. Wacker, Phys. Rev. D **76**, 055007 (2007) [arXiv:hep-ph/0506242].

[15] E. Fermi and E. Teller, Phys. Rev. 72, 399 (1947).

[16] J. Lindhard, M. Scharff and E. M. Sciott, Kgl. Danske Vikdenskab. Mat. Fys. Medd. 34 4 (1964); J. Lindhard, M. Scharff, Phys. Rev. 124 (1961) 128.

[17] K. Cheung and W. Y. Keung, Phys. Rev. D **71**, 015015 (2005) [arXiv:hep-ph/0408335].

[18] For a review, see M. J. Teper, arXiv:hep-th/9812187.

[19] A. De Roeck, J. R. Ellis, F. Gianotti, F. Moortgat, K. A. Olive and L. Pape, Eur. Phys. J. C **49**, 1041 (2007) [arXiv:hep-ph/0508198]. S. Hellman, M. Johansen, D. Milstead, ATL-PHYS-PUB 2006-015; G. Bruno (for the CMS Collaboration), CMS CR-2007/075.